MATCHING COMPUTATIONAL PREDICTIONS WITH TEMPERATURE MEASUREMENTS OF THE DUNGENESS B DOME

Mike Rabbitt[1]

[1]Thermal Hydraulics Group, Fuel and Core Branch, Technical Client Organisation, EDF, UK

ABSTRACT

This document presents a typical example of a thermo-fluids problem encountered on an Advanced Gas Cooled nuclear reactor, which is to derive the temperature distribution in the gas baffle dome at Dungeness B. It includes a comparison with measured temperatures.

1.   INTRODUCTION

The gas baffle dome at Dungeness B (Figure 1) consists of a vertical steel cylinder topped with a tori-spherical dome.
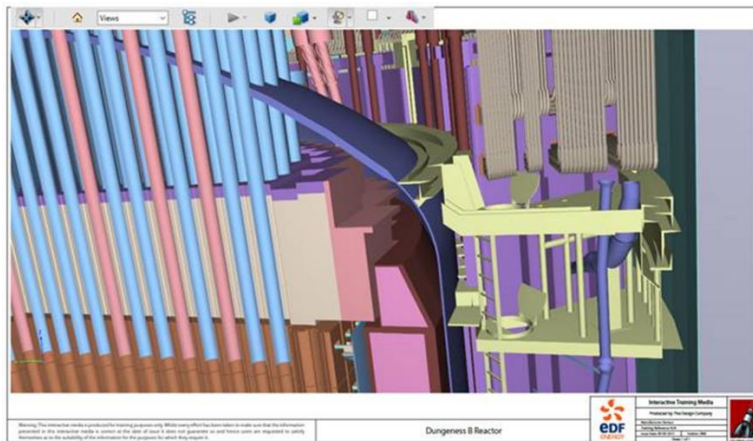
Figure 1: Image of the gas baffle and dome at DNB. The reactor is below the dome, the boiler is on the right.

It separates cool reactor inlet gas (at ~280°C) from hot reactor outlet gas (at ~630°C). The CO_2 gas pressure is ~30 bar. Below the dome, baffle boxes attach to the charge tubes (Figure 2), except for the central tubes. The boxes direct the re-entrant gas flow emanating from the gas circulators to cool the underside of the dome. The gas subsequently flows down into the core to keep the graphite moderator cool, then flows upwards and is heated by the nuclear fuel, then flows upwards inside the fuel charge tubes above the fuel, then flows into the hot box above the dome and then flows to the boilers where it is cooled.

Hot gas flows over the insulation-protected dome outer surface. 465 vertical holes pierce the dome, associated with charge tubes carrying the fuel and control rods. Each charge stub tube has a weld attaching its upper end to the outer surface of the dome at its associated hole.

The objective of the work was to provide predictions of the temperatures of all of the welds attaching all of the 465 charge tubes to the dome. This paper describes the methods adopted. There was significant time-pressure associated with the work, and the methods chosen enabled successful completion of the task in a relatively short time. All analysis was completed using FEAT (Reference 1).

*Corresponding Author: mjrabbitt@edf-energy.com

Monitoring of the dome is by a number of thermocouples measuring the temperature of both top and bottom surfaces. The variability in measured above-dome and below-dome temperature at a similar radius is significant (shown in the results section).
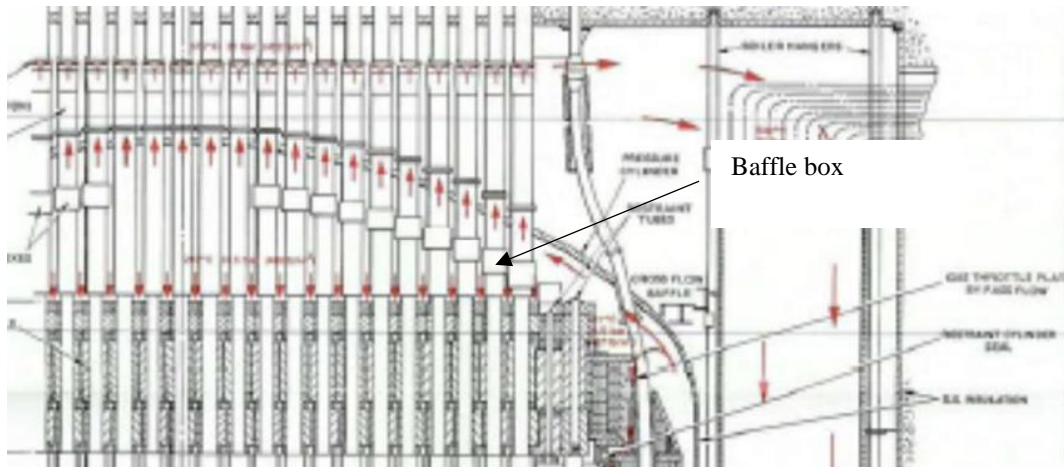
Baffle box

Figure 2 Showing the baffle boxes, which ensure effective cooling of the under-dome surface

2. UNDER-DOME HEAT TRANSFER COEFFICIENT

To predict the distribution of heat transfer coefficient on the under-dome surface requires a calculation of the gas flow in the region underneath the dome. Since the time-scale for solving the problem was short (a few weeks rather than months), building a 3-D CFD model, including in it the forest of hundreds of charge tubes and control rod guide tubes, was not achievable and instead an axi-symmetric CFD model was built.

A porous material represents the dense region containing the charge tubes under the dome; the effect of the tubes on the flow captured by a porosity distribution and appropriate flow loss coefficients. The effect of the baffle boxes is included via a separate porous material. Appropriate loss coefficients relating to flow between adjacent boxes reflect the fact that the baffle boxes are close together.

The turbulence model applied in the porous region is an eddy viscosity model for which the eddy viscosity is given by $\mu_T = \mu_{gas} + \rho q L$. q and L are representative velocity length scales for the turbulence. The energy extracted from the flow because of pressure losses is transferred into turbulence, which is a sufficient assumption to derive the average turbulence energy and hence turbulence speed. The turbulence length scale is set to the pitch of the charge tubes. The k-ε model is applied outside of the porous region, with the source term modified to ensure no unwanted production from streamline curvature.

An important part of the analysis is the calculation of heat transferred from the dome. Without modifying the turbulence length scale next to the wall, the calculated heat transfer rate is significantly too high. The value of turbulent length scale applied within the wall layer is reduced by a scaling factor to ensure that the heat transfer coefficient derived within the perforated region is the expected value. Because the flow is attached to the wall upstream of the porous region, the prediction of heat transfer at the wall in the open region is reasonably accurate.

Figure 3 shows flow vectors. There is downwards flow between the baffle boxes. However, because the flow resistance provided by the baffle boxes is relatively high, the gas flows preferentially above them rather than downwards between them until the central region is reached, where there are no baffle boxes.

The gas then flows downwards towards the top of the core. In the region underneath the baffle boxes, the gas spreads out radially, resulting in a reasonably uniform velocity profile entering the core.
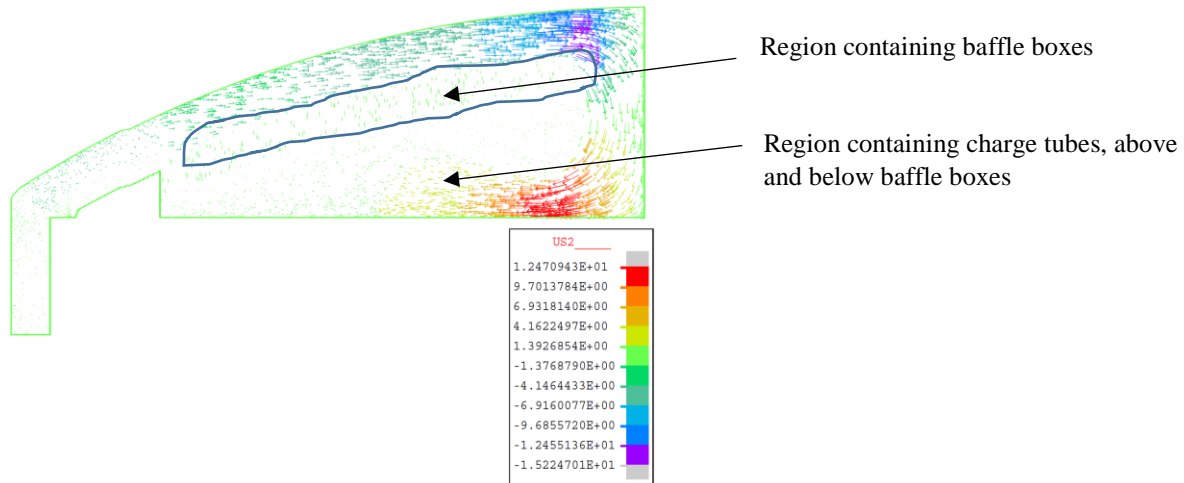
Figure 3 Flow vectors on 1% of nodes coloured on superficial radial velocity US2. A positive value indicates flow away from the dome centre, which is on the right.

Heat transfer to the dome increases as the gas enters the perforated region; the gas flow speed increases due to the reduced flow area caused by the charge tubes. Because the baffle boxes provide a significant flow resistance, only a relatively small amount of gas flow passes down between the baffle boxes, which means that most of the gas flows between the top of the baffle boxes and the dome. As the gas flows towards the centre of the dome, the cross-sectional area reduces, so the flow speed and heat transfer increases. At a radius of around 1m, the flow reaches the end of the baffle boxes and flows downwards towards the core. In this region the heat transfer to the under-side of the dome drops.

2.1   Variability

The measured thermocouple data (shown later) indicate a significant variability in under-dome-heat transfer coefficient at the same radius. This occurs because of the presence of the guide tubes. The heat transfer coefficient varies because of flow separation from the guide tubes, which inevitably leads to some regions with high heat transfer and some regions with lower heat transfer. The hottest temperatures at the same radius are in regions of lowest under-dome-heat transfer coefficient.

The difference in predictions of heat transfer coefficient distribution from two separate calculations quantifies the model variability. These two calculations differ in the value of area porosity applied in the radial direction. The two values applied are at the ends of the possible range. One is the porosity assuming the minimum gap between adjacent charge tubes and the other is the porosity from assuming the maximum gap between adjacent tubes. The local flow speed responds to the value of porosity applied, and so does the heat transfer coefficient.

Figure 4 shows the variability assumed, assuming a reactor mass flow rate relevant to full power operation.
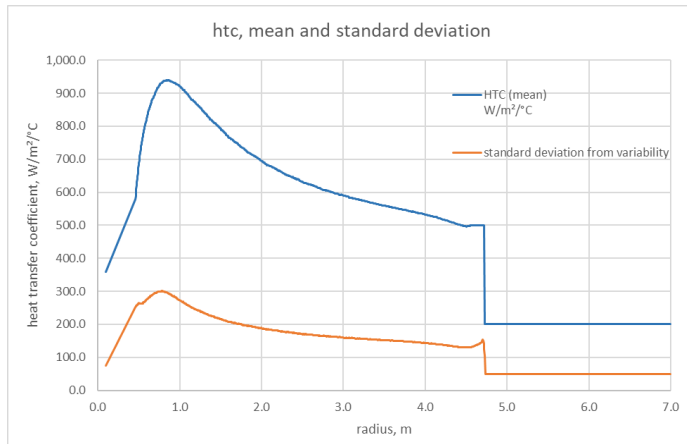
Figure 4 Predicted under dome heat transfer coefficient, mean and standard deviation

3.   DOME INSULATION CONDUCTANCE

The perforated above-dome insulation comprises multiple layers of metallic foil elements, surmounted by a cruciform-shaped cover plate. Each element contains a metallic dimpled foil sandwiched between plain foils.

Hot gas enters the permeable insulation within the central region, at the weak points in the insulation structure, which are at the charge tubes. The gas exits the insulation within the outer perforated region. The pressure drop from the centre of the hot box to the entrance of the boilers causes a flow of gas within the insulation. Gas flows radially outwards within the insulation up to the edge of the perforated region. At the radial edge of the perforated region are seals within the insulation preventing gas from flowing into the adjacent unperforated region insulation. Consequently, the gas exits the insulation as it approaches these seals, resulting in a pool of cooler temperature gas forming at the edge of the perforated region.

Heat is transferred from the flowing gas within the insulation to the metallic components of the insulation, which is then transferred to the dome by conduction. The direct transfer of heat to the dome through the gas is a relatively small contributor to the overall insulation performance.

The insulation conductance is highest within the central region. It is lower away from the central region as the gas starts exiting the insulation: heat transfer to the dome reduces because the gas temperature within the insulation is cooled by the dome upper surface, and is not replenished by any further hot gas entering the insulation.

The absolute value of conductance at each radius is estimated from the measured temperature differentials between above-dome and below-dome thermocouples. A model (not shown) also informed the distribution.

3.1   Variability

The variability assumed in the thermal performance of insulation enables consistency with plant data. Figure 5 shows the variability assumed.
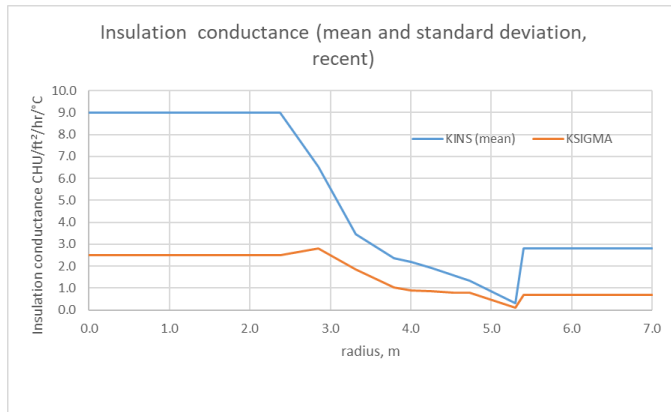
Figure 5 Predicted insulation conductance, mean and standard deviation, recent operation

3.2   Under-dome gas temperature

The CFD calculation described above confirms that the variation in under-dome gas temperature is small. The assumed gas temperature rise to the dome centre is zero.

4.   VALIDATION

Figure 6 shows the thermal solid model adopted to derive dome and stub tube temperatures at any radius.
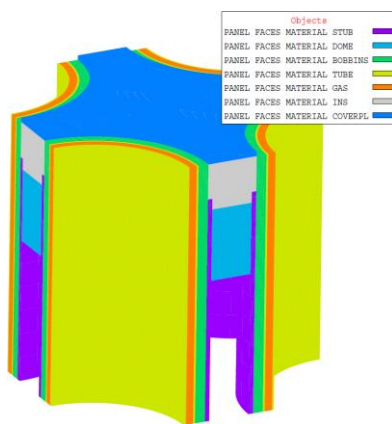
Figure 6   Thermal model of a patch of dome within four charge tubes. STUB is the stub tube, INS is the dome insulation, BOBBINS is the charge tube bobbins insulation, COVERPL is the cover-plate

To provide predictions of stub tube temperatures for the whole of the perforated region, 13 different radii are considered. The 13 radii correspond to the average radius of stub tubes within 13 radial bands. The first band contains the central tube only. The second band contains the eight tubes surrounding the inner tube. The third band contains the 16 tubes surrounding the tubes within the second band; the definition of each band proceeds like this. The thermal model is applied for each of the 13 radii, extracting the relevant values of heat transfer coefficient and insulation conductance consistent with the assumed radius.

Two sets of under-dome and above-dome thermocouple temperature predictions provide a comparison with plant data and model validation. The first set are upper bound predictions which assume the mean plus one standard deviation profile for the heat transfer coefficient and the mean minus one standard deviation profile for the insulation conductance. The second set are lower bound predictions which assume the mean minus one standard deviation profile for the heat transfer coefficient and the mean plus one standard deviation profile for the insulation conductance.

Figure 7 shows the comparison at the under- and above-dome thermocouples. The variability in measured under-dome temperatures at each radius is primarily due to the variability in under-dome-heat transfer coefficient values. The variability in measured above-dome temperatures at each radius is primarily due to the variability in under-dome heat transfer coefficient and insulation conductance values. The variability in measured temperatures at each radius is consistent with the variability in predicted temperatures.
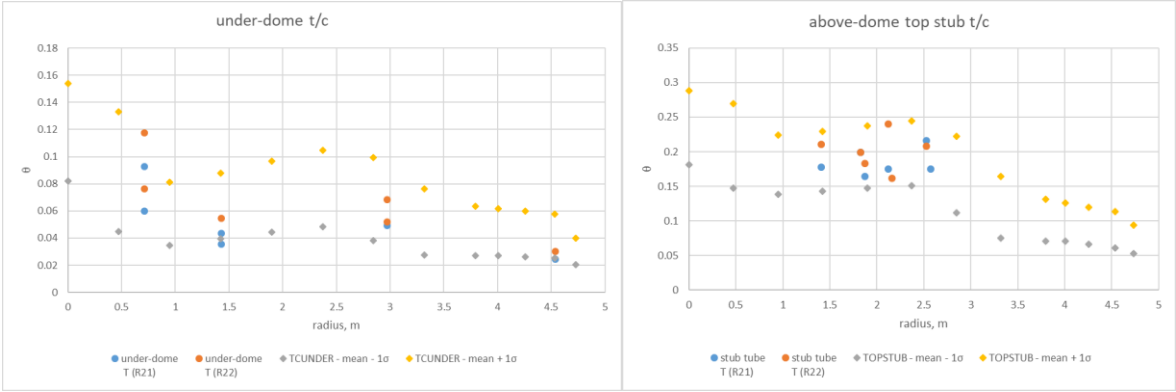
Figure 7 Comparison of predictions from the thermal model (mean ±1σ) with under-dome and above-dome measured temperatures, recent operation; dimensionless temperature.

5. DERIVING THE NUMBER OF STUB TUBES OPERATING IN EACH TEMPERATURE RANGE

A statistical model it used to determine the expected temperatures within the whole population of stub tubes. At each of the 13 different radii considered, representing tubes in a specific dome band, 1000 different calculations of the thermal model determine the distribution of temperatures; a total of 13000 calculations. Each of these calculations requires values for under-dome heat transfer coefficient and insulation conductance, obtained by random sampling from an assumed normal distribution.

The proportion of samples within each temperature range is then derived, and then multiplied by the number of tubes in that band to derive the predicted number of tubes operating in that range.
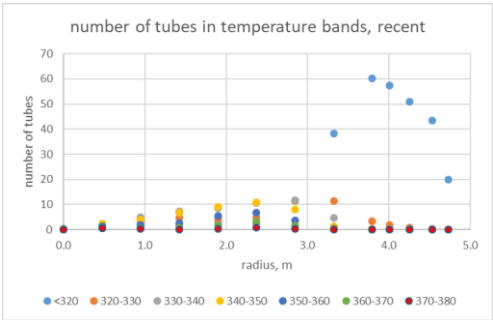
6. CONCLUSIONS

This paper has presented a pragmatic method of determining the expected number of stub tubes operating in various temperature bands. Validation of the method is by comparison with measured temperatures.

REFERENCES

[1] FEAT User Guide Version 3.23.0, March 2021, available from EDF.